Error Analysis of Various Basis Functions Used in BEM Solution of Acoustic Scattering

B. Chandrasekhar[1]

Abstract: In this work, various basis functions used in the Method of Moments or Boundary Element (MoM/BEM) solution of acoustic scattering problems are compared with each other for their performance. Single layer formulation of the rigid bodies is considered in comparison of the solutions. Geometry of a scatterer is descritized using triangular patch modeling and basis functions are defined on triangular patches, edges and nodes for three different solutions. Far field scattering cross sections for different frequencies of incident acoustic wave are compared with the closed form solutions. Also, the errors of the solutions using these three types of basis functions are computed and plotted. Finally important conclusions are drawn and future work defined.

Keywords: Acoustic scattering, Boundary Element Method, Method of moments, Error analysis, Patch based basis functions, Edge based basis functions, Node based basis functions, Boundary integral equations.

1 Introduction

With the increase in complexity of geometries like the shape and size, it becomes necessary to invent new methods to compute the acoustic fields around a scattering object faster. Though there is significant growth in the computational speeds of the computer hardware, the industry always demands solutions for larger problems which require not only the high speed processors but also the efficient and faster algorithms. Examples of the computationally large size problems include, geometries having intricate shapes like air crafts, very thin bodies like space craft wings, geometries having too many small details like engine bodies.

In a numerical method, the mathematical formulation along with the boundary conditions and geometry are descritized in order to solve the problem. The acoustic scattering problems can be solved using the numerical methods like Finite Element Method (FEM) [Frank (1998)], Boundary Element Method (BEM) [Mallardo

---

[1] Department of Mechanical Engineering, SRSIT, Bangalore

(1998), Yang (2004), Qian, Han, Ufimtsev & Atluri (2004), Yan, Cui & Hung (2005)] or method of moments solution (MoM) [Harrington (1968); Raju, Rao, & Sun (1991); Rao & Raju (1989); Rao & Sridhara (1991); Rao, Raju, & Sun (1992); and Sun & Rao (1992)], Finite Difference Method [Christopher & Ju (2009)], Mesh less Methods [Atluri (2009)] etc. Of all the numerical methods available to solve the acoustic scattering problem, Boundary Element Method (BEM) is based on integral equation formulation and the advantage of this method is reduction in dimensionality of problem. In BEM, only surface of the three dimensional object needs to be descritized compared to FEM, in which the whole volume of the domain around the scattering object is descritized. Another advantage of BEM is, radiation boundary condition is automatically implied in the formulation. BEM is also treated as one of the variants of MoM solution, which is popularly used in Electromagnetic scattering [Gibson (2007)]. Other applications of BEM can be found in ref [Tan, Shiah & Lin (2009), Soares & Vinagre (2008), Mantia & Dabnichki (2008) and Wang & Yao (2008)].

Although BEM is very popular, two major drawbacks it has are listed below. The first one being the final moment matrices becomes dense and the second one being the presence of singular, strongly singular and hyper singular kernels [De Klerk (2005)] in the boundary integral equations. To overcome the problem of dense matrices there has been a great deal of research work going on using different approaches [He, Lim & Lim (2008), Liu & Nishimura (2006), Phillips & White (1997)]. The treatment of strongly singular and hyper singular kernels has been given a great importance by the researchers to implement it numerically. Notable among them are: calculation techniques of hyper singular integrals [Yan, Hung & Zheng (2003) and Yan, Cui & Hung (2005)], derivation of non-hypersingular boundary integral equations [Qian, Han, Ufimtsev & Atluri (2004), and Qian, Han & Atluri (2004)], derivation of weekly singular and regular integrals [Han & Atluri (2007) and Sanz, Solis & Dominguez (2007)] and usage simple vector calculus operators to circumvent the hyper singularity [Chandrasekhar & Rao (2008), and Chandrasekhar (2008)] in integral equations.

In BEM, the surface of the scattering object is descritized using triangular patch modeling and it results in three types of geometric entities, namely; triangular patches, edges and nodes. The MoM/BEM solution technique has a versatile feature which allows the unknown basis functions to be defined on any of these geometric entities. The accuracy and speed of solution depends upon where the basis functions are defined. For the sake of simplicity, in this work, constant basis functions are used to compare the accuracies of the MoM/BEM solutions when the basis functions are defined on patches, edges and nodes. Rao, Raju, Sridhara, and Sun [Raju, Rao, & Sun (1991); Rao & Raju (1989); Rao & Sridhara (1991); Rao, Raju,

& Sun (1992); Sun & Rao (1992)] have used patch based constant basis functions to compute the acoustic far fields. Chandrasekhar and Rao [Chandrasekhar & Rao (2004a)] have used edge based basis functions to solve the double layer formulation since the patch based basis functions were not sufficient enough to incorporate into the solution of double layer formulation. Chandrasekhar [Chandrasekhar (2005)] developed node based basis function and advantage of using node based basis functions is it results in smallest size of moment matrix compared to edge based and patches based MoM/BEM solutions.

In this work, accuracies of the solutions based on defining the basis functions on these three geometric entities are analyzed. Comparisons are made among the solutions and the errors are computed for the cases where closed form solutions are available. Since there is no known solution available for the double layer formulation and combined layer formulation based on patch based basis function, single layer formulation is chosen for comparing the accuracies and errors of MoM/BEM solutions based on different basis functions.

2 Mathematical Formulation

Let,
(p^i, u^i) : Pressure and Velocity of the incident wave on a three-dimensional arbitrarily shaped rigid body placed in a source free homogeneous medium of density ρ and speed of sound c through the medium. Here, we note that, incident fields are defined in the absence of the scattering body,

(p^s, u^s) : Pressure and Velocity of the scattered wave and these two values depend up on the boundary condition on the scattering surface and shape of the scattering surface,

Φ : Velocity potential satisfying the Helmholtz differential equation $\nabla^2 \Phi + k^2 \Phi = 0$ for the time harmonic waves present in the region exterior to the surface S of the scattering body. The pressure and velocity fields of acoustic wave is related to the scalar velocity potential Φ as $u = -\nabla\Phi$ and $p = j\omega\rho\Phi$.

Using the potential theory and the free space Green' s function, the scattered velocity potential Φ^s for the single layer formulation may be defined as

$$\Phi^s = \int_s \sigma\left(r'\right) G\left(r, r'\right) ds' \tag{1}$$

Where
Φ^s is the scattered velocity potential,
σ is the source density function independent of r over the surface of the body,
r is the position vectors of observation point with respect to a global co-ordinate

system O,

r' is the position vectors of source point with respect to a global co-ordinate system O,

$G(r,r')$ is Free space Green's function, given by,

$$G(r,r') = \frac{e^{-jk|r-r'|}}{4\pi|r-r'|}. \tag{2}$$

$G(r,r')$ is the solution of the Helmholtz equation with a point source inhomogeneity

$$(\nabla^2 + k^2) G(r,r') = -\delta(r-r'). \tag{3}$$

For a rigid body, the normal derivative of total velocity potential, which is the sum of incident and scattered velocity potential, with respect to the observation point on the surface of the body vanishes. That is

$$\frac{\partial (\Phi^i + \Phi^s)}{\partial n} = 0 \tag{4}$$

$$\frac{\partial \Phi^s}{\partial n} = -\frac{\partial \Phi^i}{\partial n}. \tag{5}$$

where Φ^i is the incident velocity potential.

Substituting Eq. 1 into Eq. 5,

$$\frac{\partial}{\partial n} \int_s \sigma(r') G(r,r') \, ds' = -\frac{\partial \Phi^i}{\partial n}. \tag{6}$$

Eq. 6 can also be re-written as

$$\frac{\sigma(r')}{2} - \int_s \sigma(r') \frac{\partial G(r,r')}{\partial n} ds' = \frac{\partial \Phi^i}{\partial n}. \tag{7}$$

The second term in the above equation is the integration over the surface excluding the principal value term i.e. $r = r'$. We note that, this integral is a well behaved integral, although rapidly varying, which can be evaluated using standard integration algorithms.

3 Numerical Solution

Per MoM/BEM solution procedure [Harrington (1968); Chandrasekhar & Rao (2004)], Testing Eq. 7 with a testing function w_m, results in

$$\left\langle w_m, \frac{\sigma(r')}{2} \right\rangle - \left\langle w_m, \int_s \sigma(r') \frac{\partial G(r,r')}{\partial n} ds' \right\rangle = \left\langle w_m, \frac{\partial \Phi^i}{\partial n} \right\rangle. \tag{8}$$

Using the inner product definition, Eq. 8 can be written as

$$\frac{1}{2}\int_s w_m \sigma\left(r'\right) ds - \int_s w_m \int_s \sigma\left(r'\right)\frac{\partial G\left(r,r'\right)}{\partial n} ds'\, ds = \int_s w_m \frac{\partial \Phi^i}{\partial n}\, ds. \tag{9}$$

The testing functions w_m are defined on the geometric entity as similar to that of basis functions. Fig. 1 shows different geometric entities of triangular patch modeling of a geometry and basis functions are defined on each of these geometric entities in following paragraphs.
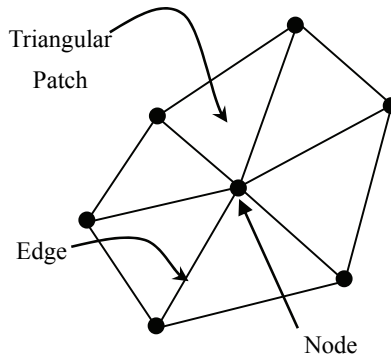
Figure 1: Triangular Patches on a Geometry

The relation between the number of patches N_f, number of edges N_e and number of nodes N_n resulted in triangular patch modeling of a closed body is $N_n - N_e + N_f = 2$ and $N_f = 2N_e/3$ [Oneill (1966)]. For example, if a closed body has 300 edges, then there will be 200 triangular patches and 102 nodes. By defining the basis functions on edges, patches and nodes, respective numerical solutions will result in moment matrices of size 300 X 300, 200 X 200 and 102 X 102.

3.1 Patch Based Basis Functions

In this case, constant basis functions are defined on the patch. Fig. 2 shows the patch T_n on which basis function is defined.

The basis function may be defined as follows:

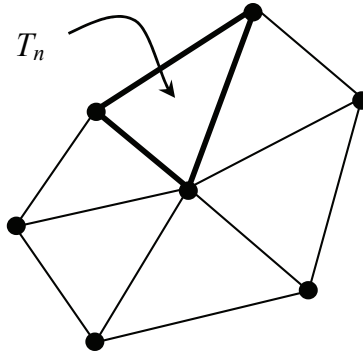$$f_n\left(r'\right) = \begin{cases} 1, & r' \in T_n \\ 0, & Otherwise \end{cases} \tag{10}$$

Figure 2: Triangular Patch on which Patch Basis Function Defined

The source density function σ over the surface of the scattering object is approximated by

$$\sigma\left(r'\right) \approx \sum_{n=1}^{N_f} \beta_n f_n \tag{11}$$

where β_n represent the unknown coefficients to be determined. In the numerical solution of Eq. 9, Galarkin's approach is used by defining the testing function in the same manner as it is defined for the basis function.

$$w_m = \begin{cases} 1, & r \in T_m \\ 0, & Otherwise \end{cases} \tag{12}$$

Substituting Eq. 12 in Eq. 9 and approximating the integrations at the centroids of triangles, Eq. 9 becomes

$$\frac{\sigma\left(r'\right)}{2}A_m - A_m \int_s \sigma\left(r'\right)\frac{\partial G\left(r_m, r'\right)}{\partial n_m}ds' = A_m\frac{\partial \Phi^i}{\partial n_m} \tag{13}$$

Where

A_m : area of triangle m,

r_m : Centroid of triangle m, and

n_m : Unit normal vector of triangle m.

Substituting Eq. 11 in Eq. 13, it results in a system of linear equations, which can be represented in the matrix form as

$$Z_P X_P = Y_P \tag{14}$$

where Z_P is the moment matrix of the single layer formulation of size $N_f X N_f$, X_P and Y_P are the column vectors of size N_f. The elements of Z_P and Y_P are given below.

$$Z_P^{mn} = \begin{cases} \frac{1}{2}A_m, & for\, m = n, \\ -A_m \int_s \frac{\partial G(r_m, r_n)}{\partial n_m} ds' & Otherwise \end{cases} \tag{15}$$

and

$$Y_P^m = A_m \frac{\partial \Phi^i}{\partial n_m} \tag{16}$$

Once the elements of the moment matrix Z_P and the forcing vector Y_P are determined, one may solve the linear system of equations, Eq. 14, for the unknown vector X_P.

3.2 Edge Based Basis Functions

In this case, basis functions are defined on the edges of the triangular patch modeling. For this, each triangular patch T_n is divided into three equal parts by joining the vertices or nodes to the centroids of triangles. For each edge n, there are two sub triangles, S_n^+ and S_n^-, attached as shown in Fig. 3.
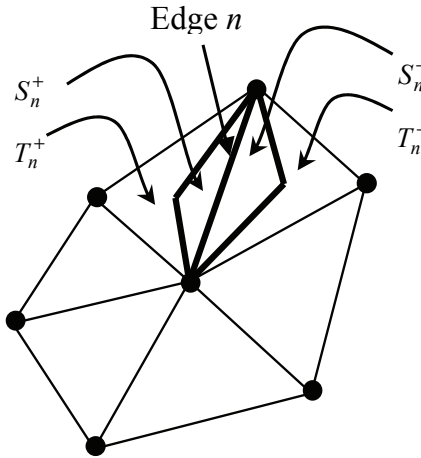

Figure 3: Adjacent Sub-Triangles on which Edge Basis Function Defined

The basis function may be defined as follows:

$$f_n(r') = \begin{cases} 1, & r' \in S_n^{\pm} \\ 0, & Otherwise \end{cases} \tag{17}$$

Following the similar procedure as discussed in previous section (Patch Based Basis Functions), the linear system of equations are derived as

$$Z_E X_E = Y_E \tag{18}$$

where Z_E is the moment matrix of the single layer formulation of size $N_e \, X \, N_e$, X_E and Y_E are the column vectors of size N_e and the elements of Z_E and Y_E are given below.

$$Z_E^{mn} = \begin{cases} \frac{1}{2} \left[\frac{A_m^+ + A_m^-}{3} \right] + \Omega_{mm}^+ + \Omega_{mm}^-, & for \; m = n, \\ - \left[\frac{A_m^+ \Omega_{mn}^+}{3} + \frac{A_m^- \Omega_{mn}^-}{3} \right], & for \; m \neq n \end{cases} \tag{19}$$

$$Y_E^m = \left[\frac{A_m^+}{3} n^+ + \frac{A_m^-}{3} n^- \right] \bullet \nabla \Phi (r_m) \tag{20}$$

where

$$\Omega_{mn}^{\pm} = \int_{S_n^+} \frac{\partial G(r_m^{\pm}, r_n^{\pm})}{\partial n_m^{\pm}} ds' + \int_{S_n^-} \frac{\partial G(r_m^{\pm}, r_n^{\pm})}{\partial n_m^{\pm}} ds'. \tag{21}$$

For more details about the derivations reader may consult ref [Chandrasekhar & Rao (2004b)].
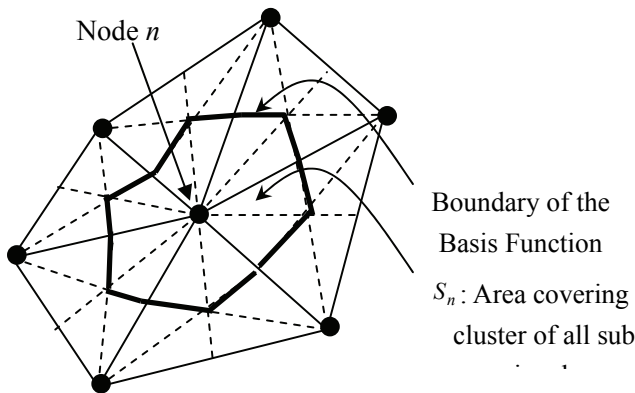
3.3 Node Based Basis Functions

Figure 4: Cluster of Sub-Triangles on which Node Basis Function Defined

In this case, basis functions are defined on the nodes, i.e. on all the sub-triangles surrounding the node n. Sub triangles are formed by joining nodes with the mid points of opposite edges as shown in Fig 4. All the sub triangles surrounding the node n are grouped into a cluster and the basis function is defined on the cluster. Let there are u number of sub triangles around field node m and v number of sub triangles around the source node n. In this paper, index x is used to represent the sub triangle attached to the field node and index y is used to represent the sub triangle attached to the source node. Let S_n represent the region of cluster on which basis function is defined. The node based basis function may be defined as

$$f_n\left(r'\right) = \begin{cases} 1 & r' \in S_n \\ 0 & Otherwise \end{cases} \tag{22}$$

Following the procedures described in previous sections, the linear system of equations are derived as

$$Z_N X_N = Y_N \tag{23}$$

where Z_N is the moment matrix of the single layer formulation of size $N_n X N_n$, X_N and Y_N are the column vectors of size N_n. The elements of Z_N and Y_N are given below.

$$Z_N^{mn} = \begin{cases} \frac{1}{2} \sum\limits_{x=1}^{u} A_m^x & for\, m = n\, and\, x = y \\ -\sum\limits_{x=1}^{u} \sum\limits_{y=1}^{v} A_m^x \int_s \frac{\partial G\left(r_m^{cx}, r_n^{cy}\right)}{\partial n_m^x} ds' & otherwise \end{cases} \tag{24}$$

and

$$Y_N^m = \sum\limits_{x=1}^{u} A_m^x \frac{\partial \Phi^i}{\partial n_m^x} \tag{25}$$

where A_m^x is the area of sub-triangle attached to the field node m, r_m^{cx} is the position vector to the centroid of xth sub-triangle attached to field node m, r_n^{cy} is the position vector to the centroid of yth sub-triangle attached to source node n, $\partial G/\partial n_m^x$ is the normal derivative of Green's function at the centroid of xth sub-triangle attached to field node m, and n_m^x is the unit normal vector of xth sub-triangle attached to the field node m. For more details about the derivations reader may consult ref [Chandrasekhar (2005) and (2008)].

Once the elements of the impedance matrices Z_P, Z_E and Z_N; and the forcing vector Y_P, Y_E and Y_N are determined, one may solve the linear system of equations, Eqs. 14, 18 and 23, for the unknown vectors X_P, X_E and X_N, respectively.

For a plane wave incidence, we set

$$\Phi^i = e^{jk\hat{k} \bullet r} \tag{26}$$

where the propagation vector $\hat{k}$ is given by,

$$\hat{k} = \sin\theta_0 \cos\phi_0 \, a_x + \sin\theta_0 \sin\phi_0 \, a_y + \cos\theta_0 \, a_z \tag{27}$$

(θ_0, ϕ_0) define the angles of arrival of the plane wave in the conventional spherical co-ordinate system and a_x, a_y and a_z are the unit vectors along the x, y and z axes, respectively.

The normal derivative of the incident field may be written as

$$\begin{aligned}
\frac{\partial \Phi^i}{\partial n} &= n \bullet \nabla \Phi^i \\
&= jkn \bullet \hat{k} e^{jk\hat{k} \bullet r}.
\end{aligned} \tag{28}$$

Here we note that, when the frequency of the incident wave is in the close vicinity of the characteristic frequency related to Dirichlet problem, the moment matrices Z_P, Z_E and Z_N becomes highly ill-conditioned and the solution vectors X_P, X_E and X_N turns out to be spurious resulting in unphysical values of source distribution σ. One may consult ref [Chandrasekhar (2004b) and (2008)] to address the resonance problem and in this work, it is only the intention to show comparison between performances of different basis functions.

4   Error Measure

The error in the acoustic scattering problem solutions based on numerical methods may arise from many sources. It can be due to triangular patch modeling or the numerical method. The size of the triangular patches generated in approximating the surface of the scatterer has an impact on the error. Higher the size of patches or lower the mesh density, higher the error, especially for geometries having curvatures. Similarly the number of triangular patches used per wavelength also plays an important role in the amount of error.

Errors in the numerical solutions also arise from the integral equation formulations like Helmholtz Integral Equation Formulation [Burton and Miller (1971)] and Layer Formulations [Chandrasekhar and Rao (2004b)], testing and basis functions, type and order of the basis functions. Since the quadrature rules are used in the solutions of integral equation formulations, the kind of rules used also contribute the error. Finally the linear system solution algorithms used, either iterative of direct solvers, may also impact the magnitude of error.

The error can also come from scatterer smoothness, fictitious internal resonances, angle of incidence, types of final numerical result like scattered field, total field, scattering cross section.

In this work, only the scattering cross sections are computed for canonical shapes which have exact solutions available. And the following relation is used in computing the error. Let S and $\hat{S}$ be the scattering cross section based on closed form solution and numerical solution respectively. The error can be estimated as

$$Error = \frac{S - \hat{S}}{S}. \tag{29}$$

There are other forms of error measurements apart from Eq. 29 for MoM/BEM based solutions and reader may refer [Warnik and Chew (2004)] for more details. The Acoustic far field scattering cross section may be expressed by the relation

$$S = 4\pi \left| \frac{\Phi^s}{\Phi^i} \right|^2 \tag{30}$$

For a canonical shaped geometries, the far field scattering cross section S based on closed form solution may be computed from the ref [Bowmen, Senior & Uslenghi (1964)], where as for the numerical solutions based on the type of basis functions used viz. Patch, Edge and Node based basis functions, the scattering cross section may be expressed as:

$$\hat{S}_P \approx \frac{1}{4\pi} \left| \sum_{n=1}^{N_f} \beta_n \left[A_n n_n \bullet r_n e^{jkn_n \bullet r_n} \right] \right|^2 \tag{31}$$

for patch based basis functions,

$$\hat{S}_E \approx \frac{1}{4\pi} \left| \sum_{n=1}^{N_e} \beta_n \left[\sum_{y=1}^{2} \frac{A_n^y}{3} n_n^y \bullet r_n^y e^{jkn_n^y \bullet r_n^y} \right] \right|^2 \tag{32}$$

for edge based basis functions,

$$\hat{S}_N \approx \frac{1}{4\pi} \left| \sum_{n=1}^{N_n} \beta_n \left[\sum_{y=1}^{v} A_n^y n_n^y \bullet r_n^y e^{jkn_n^y \bullet r_n^y} \right] \right|^2 \tag{33}$$

for node based basis functions.

While many or all the sources of errors listed in the previous paragraphs are inherent in the numerical solutions, it is the intent of this research article to compare the numerical solutions by using different types of basis functions only.

5 Numerical Results

In this section, numerical results for the case of a sphere are presented since the closed form solution is available. The numerical results based on patch, edge and node based basis functions are compared with the closed form solution and the errors are computed for different scattering directions. To begin with, a sphere of radius 1m is approximated with triangular patch modeling which results in geometric entities like triangular 352 patches, 528 edges and 178 nodes. The number of triangular patches on the surface of sphere is chosen in such way that there are at least 10 patches per unit wavelength of the incident wave. Numerical results are plotted for the same approximated geometry but by varying the frequency of the incident acoustic wave. In all cases, incident acoustic wave travels in –Z direction and center of the sphere is located at the origin of the coordinate system.

In case of edge based solution, since the basis functions are defined on edges, it results in a moment matrix of size 528 X 528. Similarly, for patch based and node based solution, the sizes of moment matrix are 352 X 352 and 178 X 178, respectively. It is clear that, computational cost of inverting moment matrix is least for the case of node based basis functions and is most for edge based basis functions.

Figs. 5 through 9 show the scattering cross section of rigid sphere of radius 1m for $k = 1\,rad/m$ through $k = 5\,rad/m$ for the polar angles 0 to $180°$. By care fully studying the plots, it can be concluded qualitatively that solutions based on edge based basis functions are more accurate compared to patch and node based solutions; and patch based solutions are more accurate than node based solutions and less accurate than edge based solutions. The reason for this kind of behavior is, since constant basis functions are defined on edges, patches and nodes, variation of source density function on the surface of the scatterer can be better represented with edge based basis functions compared to the other two as number of defined basis functions are more in this case. Similarly, since the number of patches is almost equal to two times the number of nodes, patch based basis function represent better variation of source density function on the surface of the scatterer compared to node based basis functions.

Similarly quantitative measurements of errors are plotted in Figs. 10 through 14 and it can be concluded that overall, edge based solutions have better accuracy compared to the rest two.

It can be concluded that edge based solutions are the best in terms of accuracy compared to the other two as the variation of the source density function on the surface of scatterer can be better represented due to more number of defined basis functions. However, the computational cost involved in the solution of linear system of
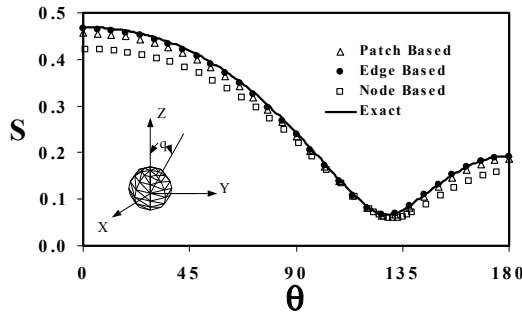
Figure 5: Scattering cross section versus polar angle for an acoustically rigid sphere of radius 1m, subjected to an axially incident plane wave of $k = 1\,rad/m$.
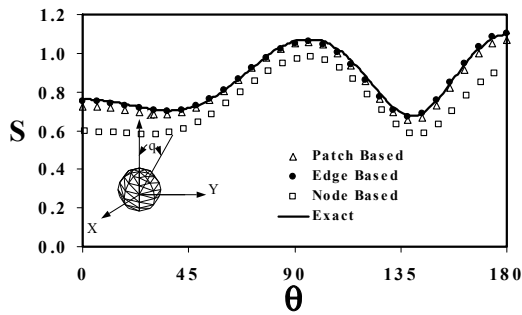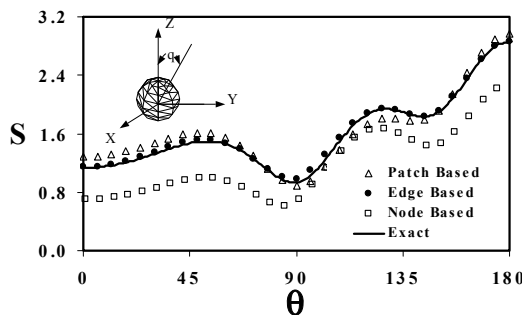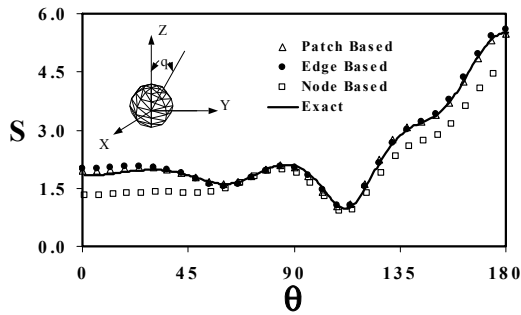

Figure 6: Scattering cross section versus polar angle for an acoustically rigid sphere of radius 1m, subjected to an axially incident plane wave of $k = 2\,rad/m$.
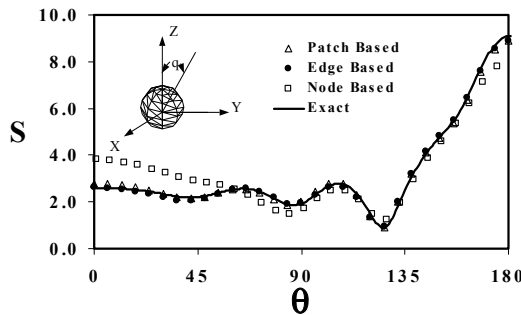

Figure 7: Scattering cross section versus polar angle for an acoustically rigid sphere of radius 1m, subjected to an axially incident plane wave of $k = 3\,rad/m$.

Figure 8: Scattering cross section versus polar angle for an acoustically rigid sphere of radius 1m, subjected to an axially incident plane wave of $k = 4\,rad/m$.

Figure 9: Scattering cross section versus polar angle for an acoustically rigid sphere of radius 1m, subjected to an axially incident plane wave of $k = 5\,rad/m$.
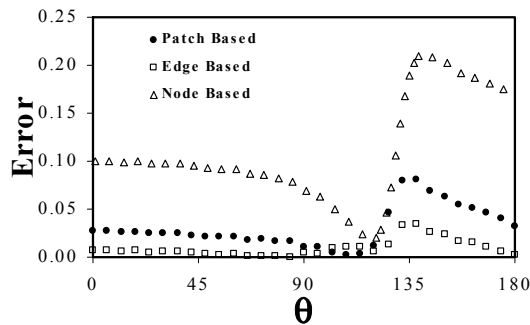

Figure 10: Back scattering amplitude error versus polar angle for an acoustically rigid sphere of radius 1m, subjected to an axially incident plane wave of $k = 1\,rad/m$.
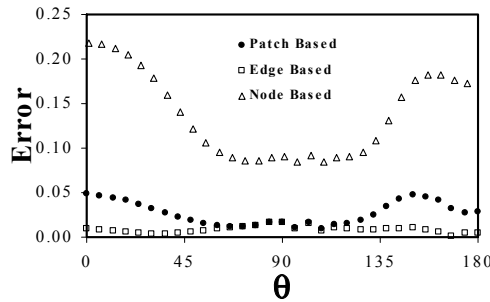
Figure 11: Back scattering amplitude error versus polar angle for an acoustically rigid sphere of radius 1m, subjected to an axially incident plane wave of $k = 2\,rad/m$.

Figure 12: Back scattering amplitude error versus polar angle for an acoustically rigid sphere of radius 1m, subjected to an axially incident plane wave of $k = 3\,rad/m$.

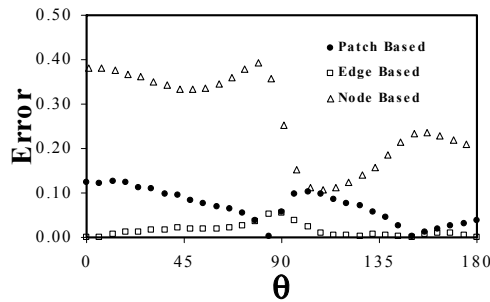Figure 13: Back scattering amplitude error versus polar angle for an acoustically rigid sphere of radius 1m, subjected to an axially incident plane wave of $k = 4\,rad/m$.
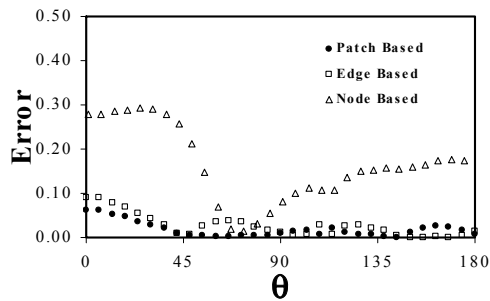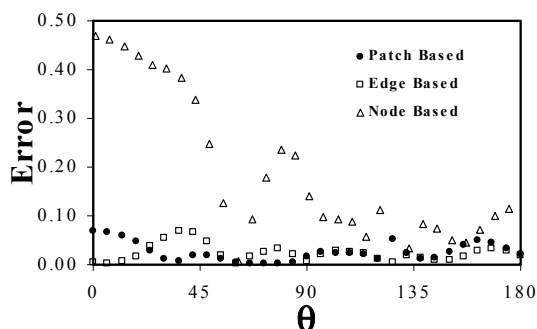
Figure 14: Back scattering amplitude error versus polar angle for an acoustically rigid sphere of radius 1m, subjected to an axially incident plane wave of $k = 5\,rad/m$.

equations is least in case node based solutions. To exploit the benefits of both less computational cost and better accuracy, one can choose the patch based solutions.

6   Conclusions

In this work, the error measurements are made for numerical solutions based on patch, edge and node based solutions. Also, the matrix equations are presented along with the size of the moment matrices generated in the solutions. It is concluded that edge based solutions are the best in terms of accuracy compared to the other two as the variation of the source density function on the surface of scatterer can be better represented due to more number of defined basis functions. However, the computational cost involved in the solution of linear system of equations is least in case node based solutions. To exploit the benefits of both less computational cost and better accuracy, one can choose the patch based solutions. But, the problem that exists with the patch based basis functions are, there is no known numerical solution available to solve the double layer formulation which is necessary to ensure a unique solution. Next level in this research work would be to develop numerical procedures to solve double layer formulation based on defining basis functions on patches.

References

Atluri S.N. (2009): The meshless method for domain and BIE descritizations, Techscience Press,USA.

Bowman J.J.; Senior T.B.A.; Uslenghi P.L.E. (1969): Electromagnetic and Acustic Scattering by Simple Shapes North-holland, Amsterdam.

Burton A.J.; Miller G.F. (1971): The application of integral equation methods to the numerical solution of some exterior boundary value problems. *Proceedings of Royal Society, London* vol A323, pp. 601-618 .

Christopher K.W.; Ju H. (2009): Finite difference computation of acoustic scattering by small surface inhomogeneities and discontinuities, *Journal of Computational Physics*, Volume 228, 16, pp 5917-5932**.**

Chandrasekhar B; Rao S.M (2004a): Acoustic scattering from rigid bodies of arbitrary shape—Double layer formulation, *The Journal of the Acoustical Society of America,* vol 115, 5, pp. 1926-1933.

Chandrasekhar B.; Rao S.M. (2004b): Elimination of internal resonance problem associated with acoustic scattering by three-dimensional rigid body, *Journal of Acoustical Society of America,* vol 115, pp. 2731-2737.

Chandrasekhar B (2005): Acoustic scattering from arbitrarily shaped three dimensional rigid bodies using method of moments solution with node based basis functions, *CMES: Computer modeling in Engineering and Sciences,* vol. 9, No. 3, pp. 243-254.

Chandrasekhar B. (2008): Node Based Method of Moments Solution to Combined Layer Formulation of Acoustic Scattering. *CMES: Computer Modeling in Engineering and Sciences*, Vol. 33, No. 3, pp. 243-268.

Chandrasekhar B.; Rao S.M. (2008): A New Method to Generate an Almost-Diagonal Matrix in The Boundary Integral Equation Formulation. *Journal of Acoustical Society of America,* Vol. 124, Issue no. 6, pp. 3390-3396.

De Klerk J.H. (2005): Hypersingular integral equations—past, present, future. *Nonlinear Analysis,* 63: 533 –540.

Frank, I. (1998): Finite Element Analysis of Acoustic Scattering (Applied Mathematical Sciences), Springer.

Gibson, W.C. (2007): The Method of Moments in Electromagnetics, Chapmen Publishers.

Harrington, R.F. (1968): Field computation by Method of Moments. *MacMillan, New York*.

Han Z.D.; Atluri S.N. (2007):A systematic approach for the development of weaklysingular BIEs, *CMES: Computer Modeling in Engineering & Sciences*, 21(1): 41-52. (9)

He X.F.; Lim K.M.; Lim S.P. (2008): Fast BEM Solvers for 3D Poisson-Type Equations. *CMES: Computer Modeling in Engineering & Sciences*, 35(1): 21-48.

Karlis G.F.; Tsinopoulos S.V.; Polyzos D.; Beskos D.E. (2008): 2D and 3D boundary element analysis of mode-I cracks in gradient elasticity. *CMES: Computer Modeling in Engineering & Sciences*, 26(3): 189-207.

Liu Y.J.; Nishimura N. (2006): The fast multipole boundary element method for potential problems: A tutorial. *Engineering Analysis with Boundary Elements*, 30(5): 371-381.

Mallardo V. (1998): Boundary Element Method for Acoustic Scattering in fluid-fluid like and fluid-solid Problems, *Journal of Sound and Vibration,* vol. 216, 3, pp. 413-434.

Mantia M.L.; Dabnichki P. (2008): Unsteady 3D boundary element method for oscillating wing. *CMES: Computer Modeling in Engineering & Sciences*, 33(2): 131-153.

O'Neill B. (1966): Elementary Differential *Geometry. Academic, New York.*

Phillips J.R.; White J.K. (1997): A precorrected-FFT method for electrostatic analysis of complicated 3-D structures. *IEEE Transactions on Computer-aided Design of Integrated Circuits and Systems*, 16(10): 1059-1072.

Qian Z.Y.; Han Z.D.; Atluri S.N. (2004): Directly derived non-hypersingular boundary integral equations for acoustic problems, and their solution through Petrov Galerkin schemes. *CMES: Computer Modeling in Engineering & Sciences* 5(6): 541-562.

Qian Z.Y.; Han Z.D.; Ufimtsev P.; Atluri S.N. (2004): Non-hypersingular boundary integral equations for acoustic problems, implemented by the collocation-based boundary element method. *CMES: Computer Modeling in Engineering & Sciences* 6(2): 133-144.

Raju P.K.; Rao S.M.; Sun S.P. (1991): Application of the method of moments to acoustic scattering from multiple infinitely long fluid filled cylinders. *Computers and Structures.* vol 39, pp. 129-134.

Rao S.M.; Raju P.K. (1989): Application of Method of moments to acoustic scattering from multiple bodies of arbitrary shape. *Journal of Acoustical Society of America.* vol 86, pp. 1143-1148.

Rao S.M.; Sridhara B.S. (1991): Application of the method of moments to acoustic scattering from arbitrary shaped rigid bodies coated with lossless, shearless materials of arbitrary thickness. *Journal of Acoustical Society of America.* vol 90, pp. 1601-1607.

Rao S.M.; Raju P.K.; Sun S.P. (1992): Application of the method of moments to acoustic scattering from fluid-filled bodies of arbitrary shape. *Communications in Applied Numerical Methods*, vol 8, pp. 117-128.

Soares Jr.D.; Vinagre, M. P. (2008): Numerical computation of electromagnetic fields by the time-domain boundary element Method and the complex variable method. *CMES: Computer Modeling in Engineering & Sciences*, 25(1): 1-8.

Sanz J.A.; Solis M.; Dominguez J. (2007): Hypersingular BEM for piezoelectric solids: formulation and applications for fracture mechanics, *CMES: Computer-Modeling in Engineering & Sciences*, 17(3): 215-229.

Sun S.P.; Rao S.M. (1992): Application of the method of moments to acoustic scattering from multiple infinitely long fluid-filled cylinders using three different formulation. *Computers and Structures*. vol 43, pp. 1147-1153.

Tan C.L.; Shiah Y.C.; Lin C.W. (2009): Stress Analysis of 3D Generally Anisotropic Elastic Solids Using the Boundary Element Method. *CMES: Computer Modeling in Engineering & Sciences*, 41(3): 195-214.

Wang H.T.; Yao Z.H. (2008): A rigid-fiber-based boundary element model for strength simulation of carbon nanotube reinforced composites. *CMES: Computer Modeling in Engineering & Sciences*, 29(1): 1-13.

Yan Z.Y.; Hung K.C.; Zheng H. (2003): Solving the hypersingular boundary integral equation in three-dimensional acoustics using a regularization relationship. *J. Acoust. Soc. Am*. 113: 2674-2683.

Yan Z.Y.; Cui F.S.; Hung K.C. (2005): Investigation on the normal derivative equation of Helmholtz integral equation in acoustics. *CMES: Computer Modeling in Engineering & Sciences,* 7(1): 97-106.

Yang S.A. (2004): An integral equation approach to three-dimensional acoustic radiation and scattering problems. *J. Acoust. Soc. Am*. 116 (3): 1372-1380.

Wanrick K.F.; Chew W.C. (2004): Error Analysis of the Moment Method, IEEE Antennas and Propagation Magazine, vol 46, 6, pp38-52.